



## GEOSCIENCES

# The Influences of Seismic Hazards for Cultural Heritage Sites: Roman City of Hierapolis

ÖZDEN SAYGILI & GULTEN POLAT

**Abstract:** Earthquakes have been responsible for the destruction of hundreds of monuments throughout human history. In this study, we tried to investigate the impact of historical and instrumental devastating earthquakes in the Roman city of Hierapolis which is one of the important cultural heritages located in the city of Denizli. In this study, the seismicity in the western Anatolian region from 7 September 2014 to 31 December 2020 was investigated to explore the b-value. The grabens in the region exhibit a low b-value with respect to the noticeable part of the Menderes Core Complex. Due to devastating earthquakes, vulnerable heritages like the Roman city of Hierapolis were seriously damaged. This paper describes the seismic behaviour of the Frontinus Gate and investigates the effects of the near field earthquakes. This analysis suggests that by using a simulating nonlinear approach it is possible to explore the seismic capacity of the historical monumental building governed by the flexural or shear failure and local overturning mechanisms. Based on the findings from this study, we can say that under a near field earthquake, increasing the vulnerability to out-of-plane failure, engineering should focus on reducing the seismic risk by adopting proper strengthening and reinforcing to prevent out-of-plane failure.

**Key words:** Dynamic analysis, numerical analysis, seismicity, the Roman City of Hierapolis.

## INTRODUCTION

The Denizli basin is situated at the junction of NW-SE trending Gediz Graben and E-W trending Büyük Menderes Graben in the eastern part of the western Anadolu (Anatolian) extensional province in western Turkey, which has been home to many civilizations during its long history and therefore has ruins of many antique cities and settlements. Most of the antique cities were destroyed by strong earthquakes that occurred in ancient times. Strong historical earthquakes in the Denizli basin caused heavy damage to antique cities in the region, namely, Hierapolis in Pamukkale, Laodikeia in Denizli city center, Colassae in Honaz, Attuda in Babadağ and Tripolis in Buldan. A strong earthquake occurred in the early seventh century AD in Lykos (Çürüksu) Valley of the Denizli area, heavily damaging the

antique cities in the region and causing people to abandon their cities. Recent archaeological excavations in Hierapolis and Laodikeia clearly revealed many relics associated with the early seventh century AD earthquake. For example, the collapse directions of columns and walls are mainly towards the NE or SW.

In addition, the Aegean Extension Zone (AEZ) is a by-product of the Eurasia-Arabia collision in general, and as a result of this collision, the compressional movement in Eastern Anatolia was moved to the west by the North Anatolian Fault (NAF) and depression trenches were formed in the region. In addition, the AEZ is a part of the Eastern Mediterranean Region where seismicity is the most active and this seismicity continues rapidly. Two main tectonic features play an important role in the neotectonic

structure of the AEZ. The first is the subduction of the Aegean Subduction Zone, located in the south of the African Plate, under the Anatolian Plate. Another important tectonic feature is the North Anatolian Fault Zone. Plate movement of western Anatolia relative to Europe can be described as a counterclockwise rotation with an average speed of 24 mm/year (McClusky et al. 2000).

The surface ruptures in the Hierapolis antique city area in the Pamukkale area prove that the Pamukkale Fault is the main active fault producing strong earthquakes in the region, and severe damage is induced by earthquakes having a magnitude 6.5 or more. However, the largest earthquake could be up to 7.1 in the Denizli Basin. Throughout history, the Hellenistic and Roman city of Hierapolis in Denizli was heavily affected by earthquakes (Figure 1a) which have occurred in this region. Considerable amount of heritage artifacts especially historical masonry buildings exhibited extreme vulnerability and suffered extensive damages. In Roman times, Hierapolis was an important Asian city and during the Early Byzantine period, the city became the metropolis of Phrygia (Leucci et al. 2013). The Frontinus Gate is a brick masonry building with its own unique cultural value situated in the Hellenistic and Roman city of Hierapolis (Figure 1b). The Gate represented an important monumental gate at the northern edge of the city (D'Andria 2001) and today it is one of the most important monuments of the Hellenistic and Roman city of Hierapolis. In 1988 the site was included in the UNESCO World Heritage List with emphasis on the extraordinary natural conditions, the Greco-Roman thermal installations, and the Christian monuments (ICOMOS 1988). The gate has three openings in squared travertine blocks, with masonry arches, flanked by two round towers. The tower and the arches are linked together.

Over time the gate suffered damages from earthquakes in the IV and VII centuries (Mighetto 1999, Valluzzi 2019). Under the directorship of Paolo Verzone from the Turin Polytechnic Institute, the Missione Archeologica Italiana (MAIER), restorations on the Frontinus Gate progressed (Mighetto 1999). Today one of the towers of the opening is still in good condition while most part of the other tower collapsed from past earthquakes and other natural disasters. Since the extensive or partially damage is a priceless loss, it is worthwhile to investigate the seismic performance of the Frontinus Gate considering the seismicity in the region in order to develop appropriate methods for preservation, restoration or rehabilitation. To construct an appropriate modelling for this heritage, knowledge of structural details, mechanical properties and seismicity of the region where the buildings were built due to their complex nonlinear seismic behaviour and geometries are required. When investigating the seismic behaviour of historical artifacts and buildings, it is difficult to understand the construction type and structural details as they are generally designed by empirical approaches. In addition, identifying the material properties is another difficulty due to destructive tests. This paper describes the seismic behaviour of the Frontinus Gate, analyzing the response of the masonry building using simulated ground motions and investigating the effects of the near field earthquakes. Due to the earthquake-induced damage of masonry heritage artifacts leading to cultural and economic losses, the investigation of the seismic behavior of historical masonry structures has been an interest to a number of experimental and analytical studies (Cakir et al. 2016, Çaktı et al. 2016, Güllü & Jaf 2016, Sadeghi & Azizi 2016, Wu et al. 2017, Ferraioli et al. 2017, Formisano et al. 2018a, Formisano et al.

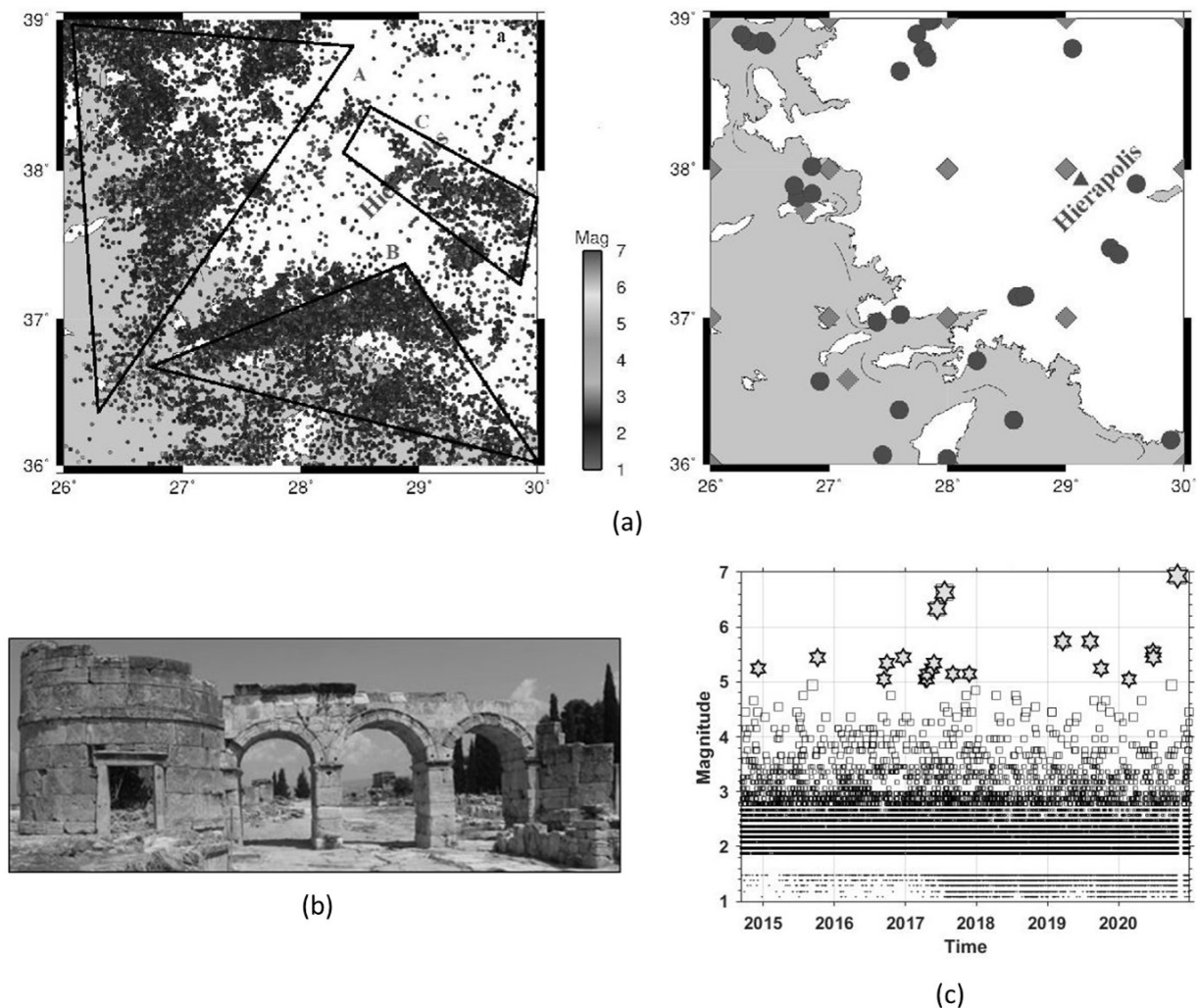


**Figure 1 (a).** Spatial distribution of local earthquakes ( $M_d \geq 1$ ) produced using the original catalog data. The color bar on the right shows the magnitudes of earthquakes. Triangle shows the location of the Roman city of Hierapolis in Denizli. The earthquake catalog of KOERI-Retmc (Bogazici University, Kandilli Observatory and Earthquake Research Institute, Regional Earthquake-Tsunami Monitoring Center) was used for this map from 7 September 2014 to 31 December 2020. Black shapes indicate subregions divided according to the earthquake clusters. Grey Circles show significant historical earthquakes based on the Ministry of Interior Disaster and Emergency Management Presidency (AFAD) and black circles represent the intermediate and larger magnitudes earthquakes. **(b)** View of the Frontinus Gate in Hierapolis. **(c)** Earthquake magnitude time series since 7 September 2014.

2018b, Yuan 2018, Chieffo et al. 2019, Saygili 2019, Xie et al. 2019; among many).

These studies have shown that historical masonry structures are vulnerable to seismic excitations compared to concrete or steel structures. Evaluation of seismic behaviour of historical masonry buildings is still a challenging task. The structural assessment of existing historical and monumental masonry buildings

requires reliable knowledge of structural details, mechanical properties and seismicity of the region where the buildings were built due to their complex nonlinear seismic behaviour and geometries. With respect to the modelling approaches, macro-modelling is a simplified but effective and reliable technique that uses an equivalent homogeneous continuum. When compared to other approaches, this technique

requires a lower computational effort. In this study a three-dimensional numerical model of the Frontinus Gate was created using a macro modelling approach with solid elements. Nonlinear dynamic analyses were performed under near field simulated ground motion data set compatible with the 2018 Turkish Building Seismic Code. For this structure to be protected in their current form and to be transferred to the future with confidence, it is important to assess their seismic performance under seismic excitations. It is intended that the interpretation of the nonlinear time history analysis results lead to contribute to protecting the cultural heritage of historical structures and their transmission to future generations.

## MATERIALS AND METHODS

### Seismicity of the region

In the regional scale, Turkey is mainly located on the Anatolian micro-plate with a small NW part in Thrace on the European Plate. The present tectonic structure of Turkey is formed by interactions between continental collision of the Arabian plate with the Eurasian plate in the east, and subduction of the African plate beneath the Aegean (McKenzie 1972, Dewey et al. 1986). Due to this, the active dynamic of the region is mainly shaped by the compression and expansion mechanism controlled by interaction among the Eurasian, Arabian and Africa plates. This effective mechanism still continues today and causes a strong seismic activity in the region as shown in Figure 1a. To investigate the seismicity of the vicinity of the Roman city of Hierapolis in Denizli limited to the coordinates of 36°-39°N, 26°-30°E, seismic b-value and  $M_c$  were computed. For seismic b-value, an earthquake catalogue prepared by KOERI-Retmc (Bogazici University, Kandilli Observatory and Earthquake Research Institute, Regional

Earthquake-Tsunami Monitoring Centre with magnitudes greater than 1.1 from 7 September 2014 to 31 December 2020 was used (Figure 1c). Figure 1c shows significant earthquakes with/without available seismic instruments which occurred in this region. As shown on Figure 1c, many serious earthquakes with magnitudes greater than 5 occurred in this region (Figure 1c). In particular, the number of such events was very high between 2017 and 2018 (Figure 1c).

The Gutenberg-Richter relation (Gutenberg & Richter 1944) and the maximum likelihood method (Aki 1965) are widely used to empirically define significant relations in seismic hazard analysis. In order to define the frequency of occurrence of earthquakes as a function of magnitude, Eq. (1) is generally used.

$$\log_{10} N = a - bM \quad \text{eq.1}$$

In Eq.(1), N represents the cumulative number of earthquakes with a magnitude greater than M where a-value and b-value are assumed to be constants. The b-value in the Gutenberg-Richter relation is unitless to measure the relative frequency of small and large earthquakes. The b-value gives information about size distribution for the relative abundance of strong to weak earthquakes. When the b-value is considered to be related to the tectonic structure of the study area, the a-value is associated with the seismic activity of the region. Therefore, the parameters give valuable information about the study area's seismic activity and tectonic regime. Firstly, seismic events (unnatural) relating to artificial quarry blasts, mine blasts from the catalogue were removed. In addition duplicate events were also removed from the catalogue. Then, the complete data set was converted to a local magnitude to ensure data set integrity. To construct this catalogue only with independent events, the catalogue was declustered by using the Reasenber (1985) algorithm. This

algorithm is a part of Stefan Wiemer's ZMAP package (Wiemer 2001). The formula used in this conversion is as provided hereinafter:

$$M_L = (0.9897 \times M_d) + 0.978$$

$R_2=0.8955$ ; *Cohesion coefficiente* (Kalafat 2016).

In this equation,  $M_d$  and  $M_L$  denote duration Magnitude and Local Magnitude, respectively.

Therefore, the final data set was evaluated as local magnitude. To determine seismic parameters (Magnitude of Completeness ( $M_c$ ), b-value and a-value), ZMAP tool (Wiemer 2001) was used. After applying declustering analysis to the catalogue, b-value, a-value,  $M_c$  for the whole region were found as 0.89, 5.796 and 1.9, respectively. Figure 2a indicates regional variations of b-value changes between 7 September 2014 and 31 December 2020 in the study area. For this analysis, the declustered earthquakes catalogue was used. The study region was additionally divided into three sub-regions to compare b and  $M_c$  values for each region (Figure 2b).  $M_c$ , b-value and a-value for each sub region A was 2.1, 0.99 and 5.607, respectively (Figure 2b). The lower seismic parameters except a-value were observed in the subregion B.  $M_c$ , b-value and a-value for the region were 1.6, 0.83 and 4.971, respectively (Figure 2b). Seismic parameters of the region C were roughly similar to the region A. The seismic parameters ( $M_c$ , b- and a-values) of the region C were 1.9, 0.89 and 4.402, respectively (Figure 2b). To get information about the physics of the earthquakes, tectonic structures and the stress distribution of the study region, b value map with the ML for 0.050 x 0.050 grid interval was computed as shown in Figure 2c. The calculated b values varied from 0.6 to 2.2 for the whole western Anatolian region. Lower b values were commonly observed in the whole region. This finding is strongly consistent with the high

seismicity of the region. The higher b values were observed in the Menderes Core Complex and surrounding area. Similar higher b values in Demirci-Gediz and Gokova Gulf-Mugla-Golhisar were determined by (Sayil & Osmaşahin 2008). In particular, the lowest b values were observed in the Kale fault (KF) and Acıgol fault (AF). Seismicity around the faults, was low according to the whole region. The findings from the seismic analysis are also consistent with heat flow measurements (Kalyoncuoglu et al. 2013). The mean value of heat flow for western Anatolia is  $107 \pm 45$  mWm<sup>-2</sup> based on silica geothermometry and  $97 \pm 27$  mWm<sup>-2</sup> for the conventional heat flow data (Ilkısık 1995).

Also, a comparison of the catalogue of 7 September 2014-31 December 2016 and 1 January 2017- 31 December 2020 was done. The number of earthquakes was gradually increased in the catalogue from 7 September 2014 to 31 December 2016. For the region we detected that  $M_c$ , b-value and a-value were 2.1, 1 and 5.699 at this time period, respectively (Figure 2c). The observed gradual increase in the number of earthquakes continued during the period from 1 January 2017 to 31 December 2020. At the time period,  $M_c$ , b-value and a-value significantly decreased.  $M_c$ , b-value and a-value were 1.8, 0.86 and 5.505, respectively (Figure 2c).

### Ground Motion Data Set

In the second half of the twentieth century, they started to use seismic records in the near field domain considering the effects of seismic ground motions on structures. It was found that the seismic motion in the near-field domain can expose structures to seismic demands different from the designed ones, both for intensity and, especially, for the nature of ground motion. The seismic ground motion in the near-field domain is mainly influenced by the fault type (e.g., strike-slip, dip-slip), by the rupture mechanism

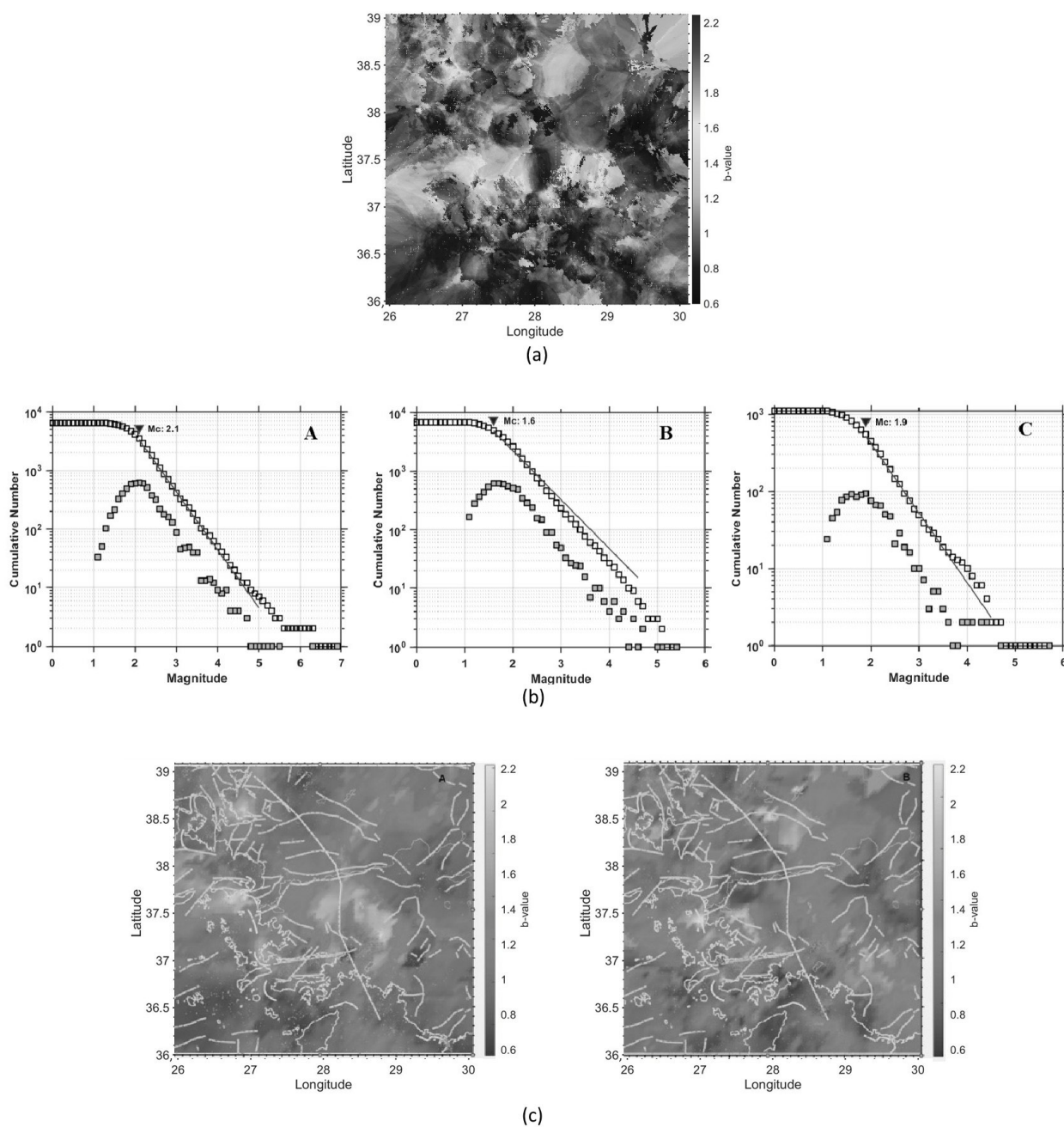


**Figure 2 (a).** b value map for the whole Western Anatolia. **(b)** Magnitude-cumulative graphs from G-R relation for three zones (A, B and C shown in Figure1a (left)) in the western Anatolia (square symbols filled with gray color are noncumulative frequency-magnitude distribution and square symbols are cumulative frequency-magnitude distribution). **(c)** b value map for the whole Western Anatolia produced by the catalogue of 7 September 2014-31 December 2016 (left). b value map for the whole Western Anatolia produced by the catalogue of 1 January 2017- 31 December 2020 (right).

(e.g., dislocation instead of crack-like rupture) and by the magnitude. Furthermore, it can also change according to the relative position with respect to the strike direction of the causative

fault. Near-field ground motions with directivity focusing or fling effects generates pulse-like ground motions with properties distinct from regular recordings (Taiyari et al. 2019, Chieffo

et al. 2020). Near fault ground motions have stronger peak ground accelerations, velocities, and displacements due to their close proximity to the rupturing fault line. Furthermore, the vertical component of a near fault ground motion is often greater than its far field counterpart.

Generally, real earthquake ground motion accelerograms as well as synthetic or artificial ground motions are employed in dynamic assessments during the evaluation of a structure's seismic response. Although recorded excitations represent the seismic action at the site as well as the source characteristics, it is often difficult to find a significant number of ground motions for seismic engineering applications. Synthetic or artificial ground motions can be employed in such cases. Synthetic ground motion generation necessitates source models that account for rupture processes, magnitude, and seismicity of the area, as well as source, route, and site impacts. The generation of artificial ground motion is based on the use of a target spectrum to match utilizing supplemental information such as time, fault distance, or peak ground acceleration (PGA). In this study, the Restricted Gutenberg-Richter Recurrence Model was used to calculate the activity of faults and to determine the probabilities of earthquake magnitudes. The probability density function developed from the Restricted Gutenberg-Richter Recurrence Model and the related cumulative distribution function were calculated. In the probabilistic seismic hazard analysis considering the probability of error in the prediction of earthquakes in the region and historical earthquakes, the maximum earthquake magnitudes of the faults in the study area and the parameters of the sources were determined using b-value and a-value.

For the target spectrum of the probability that the ground motion parameter IM will exceed a certain value of x is calculated using the total probability theorem using Eq. (3):

$$\lambda(IM > x) = \lambda(IM > m_{min}) \int_0^{m_{max}} \int_0^{r_{max}} P(IM > x | m, r) f_M(m) f_R(r) dr dm \quad 3.eq.$$

In this equation, fM (m) and fR(r) represent probability density functions of earthquake magnitude and distance, respectively. The expression P[IM > x | m, r] in the equation, which represents the probability that a certain ground motion parameter IM will exceed a certain x value for a certain distance and earthquake magnitude, is obtained from attenuation relations.

Considering the 2018 Turkish building seismic code, ground motion level that has a 2% probability to be exceeded in 50 years with return period of 2475 years was selected for this study. For this ground motion level, three sets of near field synthetic excitations were generated according to the adaptation of a random process to a target spectrum of the region. Each set of synthetic ground motions were generated for the assumption of fault distance with 3 km, 5 km and 7 km considering the effect of the Mc, b-value and a-value. These three sets include eight synthetic excitations. The correction of the random process was performed for each iteration using the Eq. (4) (Mucciarelli et al. 2004):

$$F(f)_{i+1} = F(f)_i \left[ \frac{SRT(f)}{SR(f)_i} \right] \quad 4.eq.$$

At each iteration, a Fourier transformation was applied to move from time domain to frequency domain. In order to generate the synthetic accelerogram, Gaussian white noise was multiplied by Saragoni & Hart (1974) envelope shape. Ttransient behaviour for the artificial ground motions, GM(t) the steady state motions were multiplied by Saragoni & Hart (1974) envelope shape, I(t) in which the phase angles are in the interval of [0 2π], with a uniform probability distribution Eq. (5).

$$GM(t) = I(x) \sum_i A_i \sin(w_i t + \phi_i) \quad 5.\text{eq.}$$

Soil effects were considered as linear based on NERPH class D ( $V_{s30} = 255$  m/s). The smallest and largest periods of the target response spectrum were used to determine the frequency range within the power spectral density function. In order to establish the elastic response spectra, linear dynamic analysis was performed using the Newmark integration method to solve the single degree of freedom system of equations of motion (Newmark 1959). Comparison of target spectrum and the generated near field ground motion data set for 3, 5 and 7 km are given in Figure 3.

### Seismic Response Analysis of the Frontinus Gate

A Numerical model of the Frontinus Gate was created with the well-known code SAP2000 providing 8-nodes solid finite element which activates three translational degrees of freedom at each of its connected joints. With the Finite-Element Modelling Method, SAP 2000 software enables for three-dimensional static and dynamic, linear or nonlinear, solution and dimensioning of masonry structures. It is easy to model any structural shape and produce element meshing using SAP2000 software. Spread sheets make it simple to modify or see any data, and it features automated sections and section characteristics. The FEM model of the Frontinus Gate consists of 1655 nodes and 764 Solid elements. These solid elements allow to represent three-dimensional stress conditions. One of the opening's round towers reaches a maximum height of 8.17 m. This tower's external and interior diameters are 10.20 m and 9.09 m, respectively. The other tower has a height of 3.18 m and exterior and interior diameters of 8.25 m and 7.11 m, respectively.

A numerical model of the masonry gate and the history point are depicted in Figure 4a. A finite element analysis was performed using an explicit time integration scheme to evaluate the static and seismic capacity of the masonry building. In the seismic analysis of the Gate, Young's modulus of the stone elements was taken as 2800 MPa. Material properties were determined using information inferred from previous studies (Çobanoğlu & Celik 2012, Leucci et al. 2013, Invernizzi et al. 2014, Valluzzi et al. 2019) and obvious damages. The Poisson ratio was taken as 0.24.

In order to identify the vulnerability of the building portions collapse mechanism in case of an earthquake, both linear static and modal analyses were performed. Modal analysis provided insight into the dynamic behaviour of the masonry building which was later utilized to identify the seismic response of the Gate under near field earthquakes (Figure 4b). The global translational first mode is identified by out-of-plane vibration. Second and third modes showed a similar shape to the first mode with extra oscillations of the masonry towers. The fourth mode was characterized by translational oscillations of the towers with out-of-plane bending of the masonry arches. The first modal frequency was around 10.79 Hz and corresponds to a horizontal plane bending mode shape. Second modal frequency was approximately 12.14 Hz. Mode 3 (18.34 Hz) is characterized by shear and torsional motions. The modal participation mass ratios for the first three modes were 50%, 63% and 66% respectively. The modal mass participating ratio was more than 75% at mode 10 and higher.

## RESULTS AND DISCUSSION

Static analyses provided sufficient information to identify the inadequacy in structural behaviour

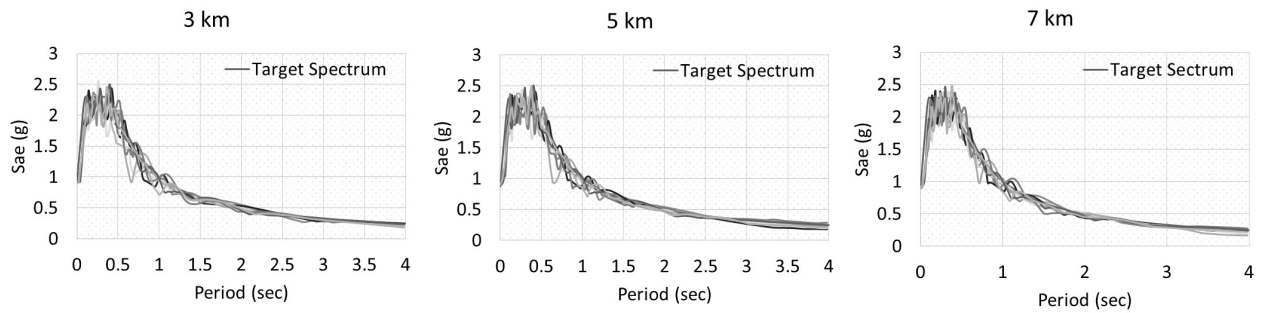


**Figure 3.** Comparison of target spectrum and generated near field ground motion data set for 3, 5 and 7 km.

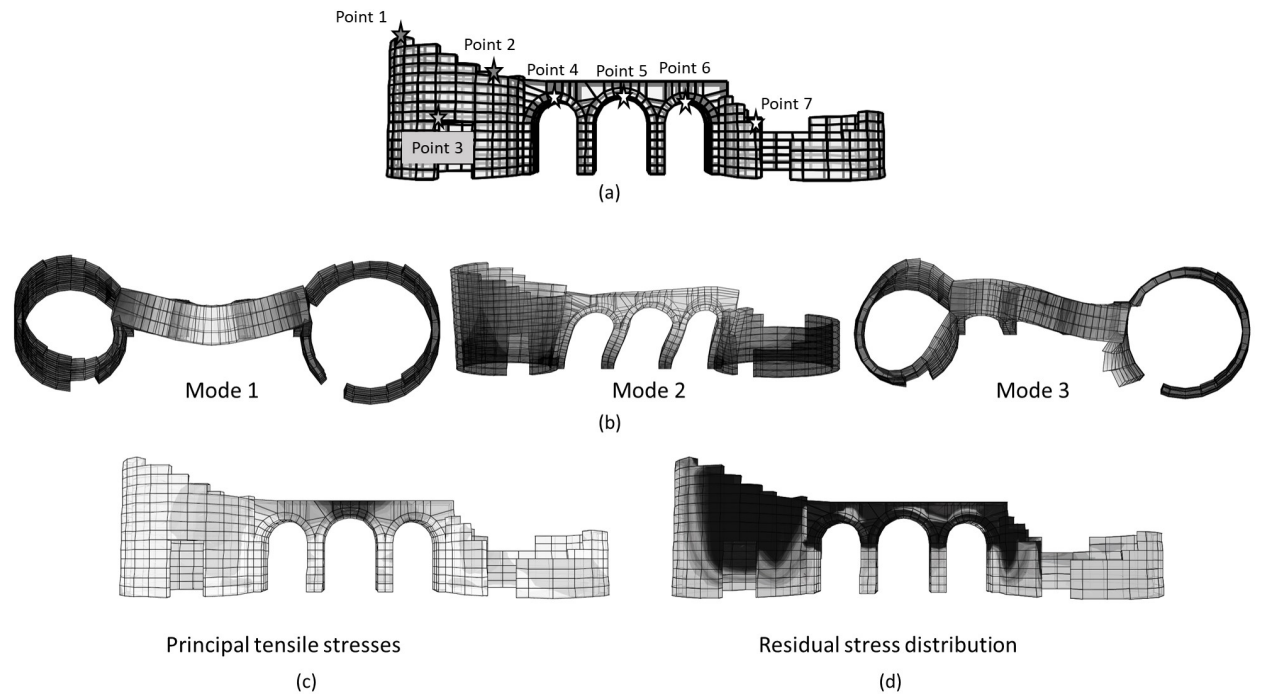


**Figure 4 (a).** Finite element model of the Frontinus Gate. **(b)** First three mode shapes of the numerical model. **(c)** Principal tensile stresses. **(d)** Residual stress distribution.

of the Gate in terms of out-of-plane bending and local deformations. Normal stresses and principle tensile stress patterns along the masonry towers and arches were about 0.3 MPa (Figure 4c). In order to investigate the dynamic global response of the Frontinus gate non-linear dynamic analyses were performed. The material uniaxial behaviour was described by a stress-strain curve using the ultimate strength of the masonry blocks in compression and tension.

Three sets of synthetic seismic excitations were applied as base excitation to the solid

finite element model. It was assumed that the structure was subjected to the earthquake in both horizontal directions. Since the seismic effects in two orthogonal directions are unlikely to reach their maximum value at the same time, the 30 percent orthogonal loading rule was applied. For each analysis, 100% of the synthetic earthquake was combined with 30% of the same motion in the orthogonal direction. The multi-linear plastic-link with pivot hysteresis type was used in order to model the shear behaviour in the time-history analyses. The link parameters that

control the stiffness degradation were chosen so as to reproduce the dynamic characteristics of the Gate and obvious damages obtained using discrete element methodology by Saygılı & Lemos (2020). The findings emphasize that the historical monument of the Frontinus Gate showed a nonlinear behaviour under near field excitations since the massive building corresponds to high inertial lateral forces. In addition, dynamic analyses results show that the towers have lower shear capacity when exposed to seismic action. The global response of the masonry gate dominated by the flexural or shear failure and local failure modes are mainly associated with the out-of-plane behaviour of tower walls. However, under 3km synthetic ground motion the Frontinus Gate showed both out-of-plane and in-plane seismic responses of tower walls simultaneously. As indicated by the analysis results, the maximum tensile and the minimum compressive principal stresses were observed along the tower and the top of the piers under 3 km, 5 km and 7 km near field excitations. A representation for the weak zones in the masonry gate under near field seismic activities is given in Figure 4d. Under three sets of the synthetic ground motions, the maximum base shear corresponded approximately to 0.28 the weight of the Gate. Under 3 km synthetic earthquakes, the masonry gate experienced highest tensile stresses which are in range of 1-2 MPa. The results highlighted that under an earthquake with a magnitude greater than 6.8 Mw, the response of the Gate would be characterized by local failures with an out of plane overturning of portions of the tower walls. In addition, variation of maximum displacements at the history points with peak ground displacement was investigated. Under ground motion data set the structure experienced large displacement which would result in the collapse behaviour. Especially under the near field ground motion

data set for 5 and 7 km there is a linear trend with the displacement and the peak ground displacement (Figure 5).

## CONCLUSIONS

The western Anatolian region is tectonically a complex area characterized mainly by extensional tectonic features and presently active subducted Hellenic and Cyprus slabs. The active tectonic units strongly influence the current seismic activity of the region. The seismicity in the western Anatolian region from 7 September 2014 to 31 December 2020 was investigated to explore the b-value. The b-value is regarded as one of the important parameters representing the nature of the occurrence of earthquakes. Particularly, the b-value characterizes the state of stress in the crust. The grabens in the region exhibit the low b-value. The conclusion of the case study of the Frontinus Gate that dates back to the 14th century allows for some general considerations about the seismicity of the region and analysis thus can be summarized as follows:

- Lower b values were observed commonly in the whole region. This finding is strongly consistent with the high seismicity of the region.
- There were higher b values in the Menderes Core Complex and surrounding area. There were similar higher b values in Demirci-Gediz and Gokova Gulf-Mugla-Göhlhisar.
- In particular, the lowest b values were observed in the Kale fault (KF) and Acıgol fault (AF).
- The findings from the seismic analysis are also consistent with heat flow measurements.
- Comparison of catalogue of 7 September 2014-31 December 2016 and 1 January 2017-31 indicates the number of earthquakes

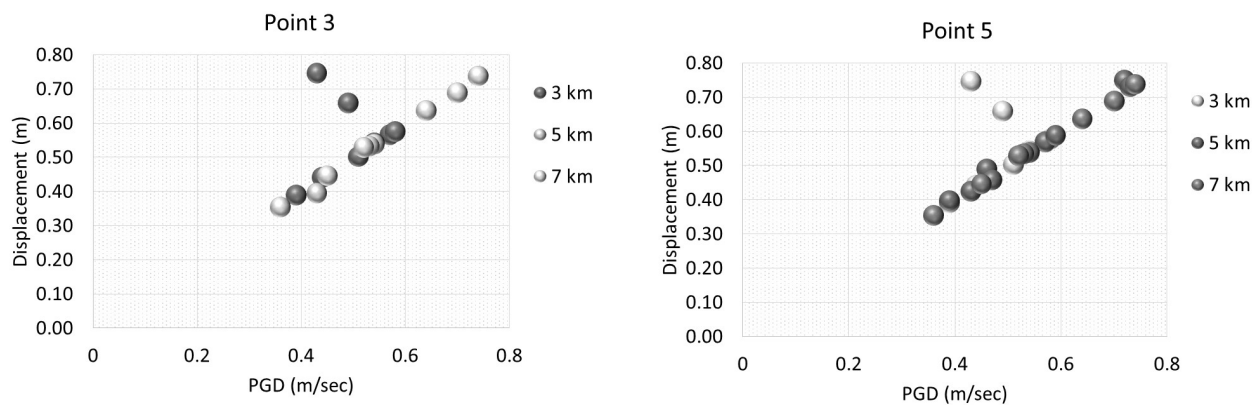


**Figure 5. Variation of maximum displacements with peak ground displacement for history points 3 and 5.**

gradually increased. This increase in the number of seismic events caused a considerable difference in seismic parameters before 2016 and after 2017.

- The numerical analyses were performed by a macro-modelling technique using a solid finite element model to simulate the nonlinear response. The seismic capacity of the historical monumental building is governed by the flexural or shear failure and local overturning mechanisms.
- Modal analysis provided insight into the dynamic behaviour of the masonry building which was later utilized to identify the seismic response of the Gate under near field earthquakes.
- Under a near field earthquake increasing the vulnerability to out-of-plane failure, engineering should focus on reducing the seismic risk by adopting proper strengthening and reinforcing to prevent out-of-plane failure.
- The results of the finite element modelling provided an insight to predict the local and global collapse mechanisms of historical masonry gate.
- By simulating a nonlinear approach, it is possible to explore the seismic capacity of the historical monumental building

governed by the flexural or shear failure and local overturning mechanisms.

- Large pulses were recorded at the beginning of the record owing to the transmission of a significant percentage of the fault's energy to the site when the fault rupture propagated towards a site with a velocity close to the shear wave velocity. Seismic waves recorded at the site with the fault's radiation pattern orientated in the fault-normal direction collide and form a massive pulse, reducing the duration of the fault waves reaching the structure. Therefore, responses under near-field ground motions distinctively have higher relative displacements between adjacent blocks as far field ground motion is concerned.
- Overturning mechanisms of masonry tower walls could be reduced or prevented by increasing the in-plane stiffness and installing connections between stones.

## REFERENCES

- AKI K. 1965. Maximum likelihood estimate of  $b$  in the formula  $\log(N) = a - bM$  and its confidence limits. *Bull Earthq Res Inst Tokyo Univ* 43: 237-239.
- CAKIR F, UCKAN E, SHEN J & AKBAS B. 2016. Seismic performance evaluation of slender masonry towers: A case study. *Struct Des Tall Build* 25(4): 193-212. doi:10.1002/tal.1235.

- ÇAKTI E, SAYGILI Ö, LEMOS JV & OLIVEIRA CS. 2016. Discrete Element Modelling of a Scaled Masonry Structure and Its Validation. *Eng Struct* 126: 224-236.
- ÇOBANOĞLU İ & ÇELİK SB. 2012. Determination of strength parameters and quality assessment of Denizli travertines (SW Turkey). *Eng Geol* 129(130): 38-47.
- CHIEFFO N, FORMISANO A & MIGUEL FERREIRA T. 2019. Damage scenario-based approach and retrofitting strategies for seismic risk mitigation: an application to the historical Centre of Sant'Antimo (Italy). *Eur J Environ Civ* 1929-1948. DOI: 10.1080/19648189.2019.1596164.
- CHIEFFO N, FORMISANO A, MOSOARCA M & LOURENÇO PB. 2020. Seismic vulnerability assessment of a romanian historical masonry building under near-source earthquake. *Proceedings of the International Conference on Structural Dynamic. EURO DYN 2*: 4957-4971.
- D'ANDRIA F. 2001. Hierapolis of Phrygia: its evolution in Hellenistic and Roman times. In *Urbanism in Western Asia Minor: New Studies on Aphrodisias, Ephesos, Hierapolis, Pergamon, Perge and Xanthos* edited by David Parrish. *J Rom Archaeol Suppl Ser* 97-115.
- DEWEY JF, HEMPTON MR, KIDD WSF, SAROGLU F & ŞENGÖR AMC. 1986. Shortening of continental lithosphere: the neotectonics of Eastern Anatolia — a young collision zone. *Geol Soc Spec Publ* 19: 1-36. <https://doi.org/10.1144/GSL.SP.1986.019.01.01>
- FERRAIOLI M, MICCOLI L, ABRUZZESE D & MANDARA A. 2017. Dynamic characterization and seismic assessment of medieval masonry towers. *Nat Hazards* 86(2): 489-515. doi:10.1007/s11069-016-2519-2.
- FORMISANO A, DI LORENZO G, LANDOLFO R & MAZZOLANI FM. 2018a. Seismic-volcanic vulnerability and retrofitting of a cultural heritage masonry palace in the Vesuvius area. *Int J Mason Res* 3(3): 244-268. DOI: 10.1504/IJMRI.2018.093485.
- FORMISANO A, KRSTEVSKA L, DI LORENZO G, LANDOLFO R & TASHKOV L. 2018b. Experimental ambient vibration tests and numerical investigation on the Sidoni Palace in Castelnuovo of San Pio (L'Aquila, Italy). *Int J Mason Res Innov* 3(3): 269-294. DOI: 10.1504/IJMRI.2018.093487.
- GUTENBERG R & RICHTER CF. 1944. Frequency of earthquakes in California. *Bull Seismol Soc Am* 34: 185-188.
- GÜLLÜ H & JAF HS. 2016. Full 3D nonlinear time history analysis of dynamic soil-structure interaction for a historical masonry arch bridge. *Environ Earth Sci* 75(21): 1421. doi:10.1007/s12665-016-6230-0.
- ICOMOS 1988. Advisory Body Evaluation, World Heritage List nomination 485 - Hierapolis- Pamukkale. p. 617.
- ILKİSİK OM. 1995. Regional heat flow in western Anatolia using silica temperature estimates from thermal springs. *Tectonophysics* 244: 175-184.
- INVERNIZZI S & ALFERI C. 2014. Combined laser surveying and finite element modelling for the structural assessment of masonry structures at the Hierapolis outer bath complex. SAHC2014 - 9th International Conference on Structural Analysis of Historical Constructions In: Peña F & Chávez M (Eds.), Mexico City, Mexico, p. 1-12.
- KALYONCUOĞLU UY, ELİTOK Ö & DOLMAZ MN. 2013. Tectonic implications of spatial variation of b-values and heat flow in the Aegean region. *Mar Geophys Res* 34: 59-78 (2013). <https://doi.org/10.1007/s11001-013-9174-8>
- LEUCCI G, DI GIACOMO G, DITARANTO I, MICCOLI I & SCARDOZZI G. 2013. Integrated ground-penetrating radar and archeological surveys in the ancient city of Hierapolis of Phrygia (Turkey). *Archaeol Prospect* 20: 285-301. doi:10.1002/arp.1461.
- MCKENZIE D. 1972. Active Tectonics of the Mediterranean Region. *Geophys J Int* 30(2): 109-185. <https://doi.org/10.1111/j.1365-246X.1972.tb02351.x>.
- MCCLUSKY S ET AL. Global positioning system constraints on plate kinematics and dynamics in the Eastern Mediterranean and Caucasus. *J Geophys Res* 105(2000): 5695-5719.
- MIGHETTO P. 1999. La storia come scavo della realtà architettonica. Paolo Verzone (1902-1986): un percorso di ricerca Politecnico di Torino. p. 1-196.
- MUCCIARELLI M, SPINELLI A & PACOR F. 2004. Un programma per la generazione di accelerogrammi sintetici "fisici" adeguati alla nuova normativa. *Proceedings of XI Congresso Nazionale L'Ingegneria Sismica in Italia*, Genova, Italy.
- NEWMARK NM. 1959. A method of computation for structural dynamics. *J Eng Mech ASCE* 85(3): 67-94.
- REASENBERG P. 1985. Second-order moment of central California seismicity: 1969-1982. *J Geophys Res* 90: 5479-5495.
- SADEGHI A & AZIZI M. 2016. Seismic vulnerability of St Stepanos Church., The second bilateral seminar between Iran and Japan Seismology and Earthquake engineering of Historical Masonry Buildings, Tabriz, Iran.
- SARAGONI GR & HART GC. 1974. Simulation of artificial earthquakes. *Earthq Eng Struct Dyn* 2: 219-267.
- SAYGILI Ö. 2019. Estimation of Structural Dynamic Characteristics of the Egyptian Obelisk of Theodosius. *Earthq Struct* 16 (3) 311-320.

SAYGILI Ö & LEMOS JV. 2020. Investigation of the structural dynamic behaviour of the Frontinus Gate. *Appl Sci* 10: 5821. doi:10.3390/app10175821.

SAYIL N & OSMANŞAHİN İ. 2008. An investigation of seismicity for western Anatolia. *Nat Hazards* 44: 51-64. <https://doi.org/10.1007/s11069-007-9141-2>.

TAIYARI F, FORMISANO A & MAZZOLANI FM. 2019. Seismic Behaviour Assessment of Steel Moment Resisting Frames Under Near-Field Earthquakes. *Int J Steel Struct* 19(5): 1421-1430. DOI: 10.1007/s13296-019-00218-2.

VALLUZZI MR, MARSON C, TAFFAREL S, SALVALAGGIO M, DEIANA R & BOAGA J. 2019. Structural investigation and modelling of seismic behaviour on ruins in the monumental area of hierapolis of Phrygia. *Structural Analysis of Historical Constructions: An Interdisciplinary Approach*. RILEM 18: 1849-1857.

WIEMER S. 2001. A software package to analyze seismicity: ZMAP. *Seismol Res Lett* 72: 373-382.

WU F, WANG H T, LI G, JIA J Q & LI H N. 2017. Seismic performance of traditional adobe masonry walls subjected to in-plane cyclic loading. *Mater Struct* 50(1): 69. doi:10.1617/s11527-016-0927-0.

XIE O, XU D, WANG Y, ZHANG L & XIN R. 2019. Seismic behaviour of brick masonry walls representative of ancient Chinese Pagoda walls subjected to in-plane cyclic loading. *Int J Archit* 1336-1348 DOI: 10.1080/15583058.2019.1674943.

YUAN JL. 2018. Analytical method on horizontal earthquake action of ancient masonry pagoda. *Earthq Eng Struct Dyn* 38(2): 18-27.

#### How to cite

SAYGILI Ö & POLAT G. 2022. Seismic Hazard's Influences for Cultural Heritage Sites: Roman City of Hierapolis. *An Acad Bras Cienc* 94: e20210487. DOI 10.1590/0001-3765202220210487.

*Manuscript received on April 01, 2021;  
accepted for publication on December 08, 2021*

#### ÖZDEN SAYGILI<sup>1</sup>

<https://orcid.org/0000-0001-7135-2511>

#### GULTEN POLAT<sup>2</sup>

<https://orcid.org/0000-0002-6956-7385>

<sup>1</sup>Yeditepe University Istanbul, Department of Civil Engineering, 26 Ağustos Yerleşimi, Kayışdağı Cad. 34755 Ataşehir, İstanbul, Turkey

<sup>2</sup>Yeditepe University Istanbul, Department of Civil Engineering, 26 Ağustos Yerleşkesi, İnönü Mahallesi, Kayışdağı Caddesi, 34755, Ataşehir, İstanbul, Turkey

Correspondence to: **Gulten Polat**  
E-mail: [gulten.polat@yeditepe.edu.tr](mailto:gulten.polat@yeditepe.edu.tr)

#### Author contributions

O.S. and G.P. carried out the analysis and interpretation of the ground motion data and the seismic data, respectively. O.S. and G.P. contributed to the conception and design of the paper. G.P. and O.S. are also responsible for the final approval and accountability, and accuracy. All authors read and approved the final manuscript.

